Distinct drivers of recent seasonal precipitation increase over Central Asia: roles of anthropogenic aerosols and greenhouse gases

Jianing Guo[1,2], Xiaoning Xie[1], Gunnar Myhre[3], Drew Shindell[4], Alf Kirkevåg[5], Trond Iversen[5,6], Apostolos Voulgarakis[7,8], Toshihiko Takemura[9], Ke Shang[10], Xinzhou Li[1], Zhengguo Shi[1], Yangang Liu[11], Xiaodong Liu[1,2], Hong Yan[1]

[1]State Key Laboratory of Loess Science, Institute of Earth Environment, Chinese Academy of Sciences, Xi'an, China
[2]University of Chinese Academy of Sciences, Beijing, China
[3]CICERO - Center for International Climate Research, Oslo, Norway
[4]Nicholas School of the Environment, Duke University, Durham, NC, USA
[5]Norwegian Meteorological Institute, Oslo, Norway
[6]Department of Geosciences, University of Oslo, Oslo, Norway
[7]Department of Physics, Imperial College London, South Kensington Campus, London, UK
[8]School of Environmental Engineering, Technical University of Crete, Chania, Crete, Greece
[9]Climate Change Science Section, Kyushu University, Fukuoka, Japan
[10]School of Civil Aviation, Xihang University, Xi'an, China
[11]Environmental and Climate Sciences Department, Brookhaven National Laboratory, Upton, NY, USA

Correspondence to: Xiaoning Xie (xnxie@ieecas.cn)

Abstract. Observational evidence reveals a pronounced wetting trend over Central Asia in recent decades, with the most substantial increases occurring during winter and summer. Yet the extent to which the drivers of these changes differ seasonally remains unknown. Here, we use single-forcing experiments from the Precipitation Driver and Response Model Intercomparison Project (PDRMIP) to examine the effects of various external forcings on winter and summer precipitation across Central Asia and to explore the physical mechanisms underlying seasonal precipitation changes. We find that greenhouse gas (GHG) forcing mainly increases winter precipitation by enhancing atmospheric moisture content through warming. In contrast, in summer, Asian sulfate aerosols enhance precipitation by modulating the westerly jet, which strengthens atmospheric moisture transport into the region. Asian black carbon exerts an opposing influence that partially offsets the sulfate-induced effect. Further attribution analysis based on CMIP6 simulations reinforces these sensitivity results and shows that GHG forcing is the primary driver of winter precipitation increases whereas anthropogenic aerosols dominate summer trends. Future CMIP6 projections suggest that under moderate- to high-emission scenarios, winter precipitation will continue to rise due to increasing GHG concentrations, while summer precipitation may decline across much of Central Asia as a result of reduced aerosol emissions following Asian clean air policies. These findings highlight a distinct seasonality in the drivers of recent

precipitation increase and suggest a plausible divergence in future winter and summer precipitation trends.

1 Introduction

Central Asia, located in the mid-latitude westerly-dominated areas of the Northern Hemisphere, is a typical arid and semi-arid region characterized by scarce precipitation (Lioubimtseva and Henebry, 2009). Under global climate change, the regional precipitation changes profoundly impact local ecological stability, agricultural production, and socio-economic development (Gessner et al., 2013; Reyer et al., 2017). In recent decades, observational evidence indicates that Central Asia has experienced significant wetting, particularly in winter and summer (Chen et al., 2011; Li et al., 2016; Hu et al., 2017; Peng and Zhou, 2017; Ma et al., 2020).

Many previous studies showed that human activities play a crucial role in recent wetting over Central Asia, as a result of increased levels of greenhouse gases (GHGs) (mainly CO_2 and CH_4), and anthropogenic aerosols (Peng et al., 2018; Dong et al., 2022; Xie et al., 2022; Fallah et al., 2023). Increasing GHG concentrations induced by anthropogenic emissions have driven global warming, which tends to intensify the global hydrological cycle (Held and Soden, 2006; Oki and Kanae, 2006). The warming-induced increases in oceanic evaporation and water vapor transport lead to enhancements in mean and extreme precipitation in Central Asia (Chen et al., 2011; Peng and Zhou, 2017; Wang et al., 2017; Yang et al., 2020). Furthermore, the warming rate in the past three decades is significantly higher than the rate of global mean surface temperature increase of about 0.39 °C decade^{-1} (Vose et al., 2012; Hu et al., 2014), which accelerates regional snow and glacier melting in high-mountain Asia and increases regional precipitation (Kraaijenbrink et al., 2021; Zhang et al., 2022). Besides GHGs, anthropogenic aerosols influence the Earth's energy budget through absorbing and scattering shortwave and longwave radiation, and interacting with clouds as well (Rotstayn and Lohmann, 2002; Ramanathan and Carmichael, 2008; Shindell and Faluvegi, 2009; Booth et al., 2012; Bond et al., 2013; Myhre et al., 2017; Jia et al., 2021). These aerosol-radiation and aerosol-cloud interactions not only impact local precipitation but also induce remote precipitation responses through large-scale atmospheric circulation modulation (Shindell et al., 2012; Myhre et al., 2013; Shawki et al., 2018; Undorf et al., 2018; Westervelt et al., 2018; Guo et al., 2024). Owing to industrialization and urbanization in Asian developing nations since the 1980s, anthropogenic aerosol emissions from East and South Asia have

risen substantially (Ohara et al., 2007; Lu et al., 2011). Several studies indicate that increased Asian anthropogenic aerosols drive a meridional shift of the Asian subtropical westerly jet in summer, which potentially affects precipitation in Central Asia (Dong et al., 2022; Xie et al., 2022). In addition, internal variability, such as interdecadal variations in Atlantic and Pacific sea surface temperature, can also contribute to the regional precipitation changes in Central Asia (Huang et al., 2013; Gerlitz et al., 2016; Jiang et al., 2021).

It is noted that previous studies have mainly focused on annual precipitation changes in historical and future times and the corresponding physical drivers (Chen et al., 2011; Huang et al., 2014; Li et al., 2016; Hu et al., 2017; Jiang et al., 2020). However, it remains unknown whether seasonal differences exist in the drivers of regional precipitation change. In this study, we employ idealized single-forcing sensitivity experiments from the Precipitation Driver and Response Model Intercomparison Project (PDRMIP) to examine the seasonal precipitation changes and associated mechanisms in response to GHG and anthropogenic aerosol forcings in Central Asia, particularly in winter (December–February, DJF) and summer (June–August, JJA). Combined with multi-model simulations from the Coupled Model Intercomparison Project Phase 6 (CMIP6), we assess the responses of winter and summer precipitation changes to external forcings in the historical simulations over Central Asia, and further reveal possible future trends in winter and summer precipitation under different emission scenarios.

2 Data and Methods

2.1 Observed datasets

The Global Precipitation Climatology Project (GPCP) dataset, which integrates multiple satellite measurements and rain-gauge observations (Adler et al., 2003), provides long-term global precipitation data and has been widely used to study precipitation changes in Central Asia (Yu et al., 2018; Ma et al., 2020; Yang et al., 2020; Liu et al., 2022). In this study, the GPCP Version 2.3 monthly dataset (Adler et al., 2018), spanning 1979–2014 with a 2.5°×2.5° horizontal resolution, is utilized to investigate the observed seasonal precipitation trends in Central Asia (35°N–50°N, 65°E–90°E). We also utilize gauge-based gridded precipitation datasets to examine the precipitation trends, including the Global Precipitation Climatology Center (GPCC) with a horizontal resolution of 0.25°×0.25° from 1950 to 2019 (Schneider et al., 2020), and the Climatic Research Unit (CRU) with a horizontal resolution of

0.5°×0.5° from 1950 to 2024 (Harris et al., 2020). ERA5 zonal wind at 200 hPa is used to analyze changes in the Central Asian summer westerly jet during 1979–2025 (Hersbach et al., 2020).

2.2 PDRMIP simulations

Multi-model simulations from the PDRMIP are utilized to explore the impacts of several external forcing factors on seasonal precipitation in Central Asia and identify the underlying physical mechanisms (Myhre et al., 2017, 2022). Detailed information on the PDRMIP models used in this study is summarized in the supplement (Table S1). Baseline experiments were conducted using nine GCMs under year 2000 anthropogenic and natural forcing conditions, with different conditions for HadGEM2 (Stjern et al., 2017). Three global-scale perturbation experiments include doubling CO_2 concentrations (CO_2x2), tripling CH_4 concentrations (CH_4x3), and increasing solar irradiance by 2% (Solar+2%). Two regional aerosol perturbation experiments involve increasing Asian sulfate concentrations or emissions by a factor of 10 (Sulx10Asia) and increasing Asian black carbon (BC) concentrations or emissions by a factor of 10 (BCx10Asia). All the models incorporated aerosol direct effects and BC semi-direct effects, and some of these models adopted full microphysics parameterizations of aerosol-cloud interactions (Myhre et al., 2017; Liu et al., 2018). The climate responses to various external forcings were evaluated by nine models for CO_2x2, CH_4x3, and Solar+2% forcings, seven models for Sulx10Asia forcing, and six models for BCx10Asia forcing (Supplement Table S2). All numerical experiments were conducted including the coupled ocean-atmosphere simulations (except for NCAR-CESM1-CAM4, with a slab ocean) and fixed-SST simulations. The coupled ocean-atmosphere simulations were run for at least 100 years, with the last 50 years used for analysis. Fixed-SST simulations were performed for at least 15 years, with the last decade used for analysis. These fixed-SST simulations are used to estimate effective radiative forcing (ERF) of external forcings, calculated as top-of-atmosphere net radiative flux differences between baseline and perturbation experiments (Hansen et al., 2005; Myhre et al., 2013; Forster et al., 2016; Smith et al., 2020). Compared to instantaneous radiative forcing, ERF additionally includes rapid adjustments in the forcing estimate, such as cloud adjustments (from atmospheric temperature and aerosols), fast land surface responses, and tropospheric temperature and humidity changes (Hansen et al., 2005; Boucher et al., 2013; Myhre et al., 2013; Forster et al., 2016; Bellouin et al., 2020; Smith et al., 2020). Vertical coordinates were transformed to a 17-level pressure coordinate system to enable multi-model averaging.

2.3 CMIP6 simulations

To examine the attribution of historical precipitation changes and compare with observations, we utilize multi-model simulations from the Detection and Attribution Model Intercomparison Project (DAMIP) in CMIP6 (Gillett et al., 2016). Our analysis includes all-forcing historical simulations, simulations with only well-mixed GHGs (hist-GHG), simulations with only anthropogenic aerosols (hist-aer), and simulations with only natural factors of solar activity and volcanic forcing (hist-nat) in DAMIP. For future projections, we use three Shared Socioeconomic Pathways (SSPs: SSP2-45, SSP3-70, and SSP5-85) from the Scenario Model Intercomparison Project (ScenarioMIP; O'Neill et al., 2016; Eyring et al., 2016) in CMIP6. The medium GHG emission scenario (SSP2-45) assumes moderate climate mitigation measures. The high GHG emission scenarios (SSP3-70 and SSP5-85) represent limited climate policy intervention in the future. Table S3 in the supplement summarizes the models utilized in the CMIP6 analysis. We calculated precipitation trends over Central Asia separately for summer and winter during historical (1979–2014) and future (2015–2100) periods. Both for PDRMIP and for CMIP6 outputs, the data were interpolated to a 2.5°×2.5° horizontal resolution using bilinear interpolation.

3 Results

3.1 Observational seasonal precipitation trends

We examine the temporal and spatial characteristics of seasonal precipitation in Central Asia derived from GPCP. Figure 1a shows annual and seasonal trends of the regionally averaged observed precipitation over Central Asia from 1979 to 2014. The annual precipitation change exhibits a statistically significant increasing trend of 0.23 mm day^{-1} per 100 years. Among the four seasons, summer and winter precipitation show more significant increases, with linear trends of 0.41 mm day^{-1} per 100 years for summer and 0.35 mm day^{-1} per 100 years for winter, respectively. Spring precipitation shows a small negative trend, and autumn exhibits a slight increase. Based on the annual or seasonal precipitation trend values from all grid points within the study region, a normal distribution is fitted to obtain the corresponding probability density function (PDF) curves. The PDFs (Fig. 1b) and spatial distribution of precipitation trends (Figs. 1c–e) indicate that the precipitation significantly increases across most regions of Central Asia during summer and winter, with insignificant precipitation changes in spring and autumn (Supplement Fig. S1). The spatial distributions of annual, summer, and winter precipitation trends derived from GPCC and CRU show positive precipitation trends over Central Asia in Supplement Fig. S2. The summer and winter increases dominate the annual

precipitation changes in Central Asia, consistent with other observed precipitation datasets (Chen et al., 2011; Li et al., 2016; Hu et al., 2017; Peng and Zhou, 2017; Ma et al., 2020). Supplement Fig. S3 shows the southward shift of the westerly jet during 1979–2014, which is closely associated with the summer wetting trend over Central Asia (Zhao et al., 2014; Peng and Zhou, 2017; Peng et al., 2018). Additionally, we also examine the precipitation trends calculated as the relative change per decade (unit: % decade^{-1}) in Supplement Fig. S4. The higher value of the positive trends over the arid region of northwestern China indicates a significant regional wetting during recent decades, larger than 12% decade^{-1} for annual precipitation.

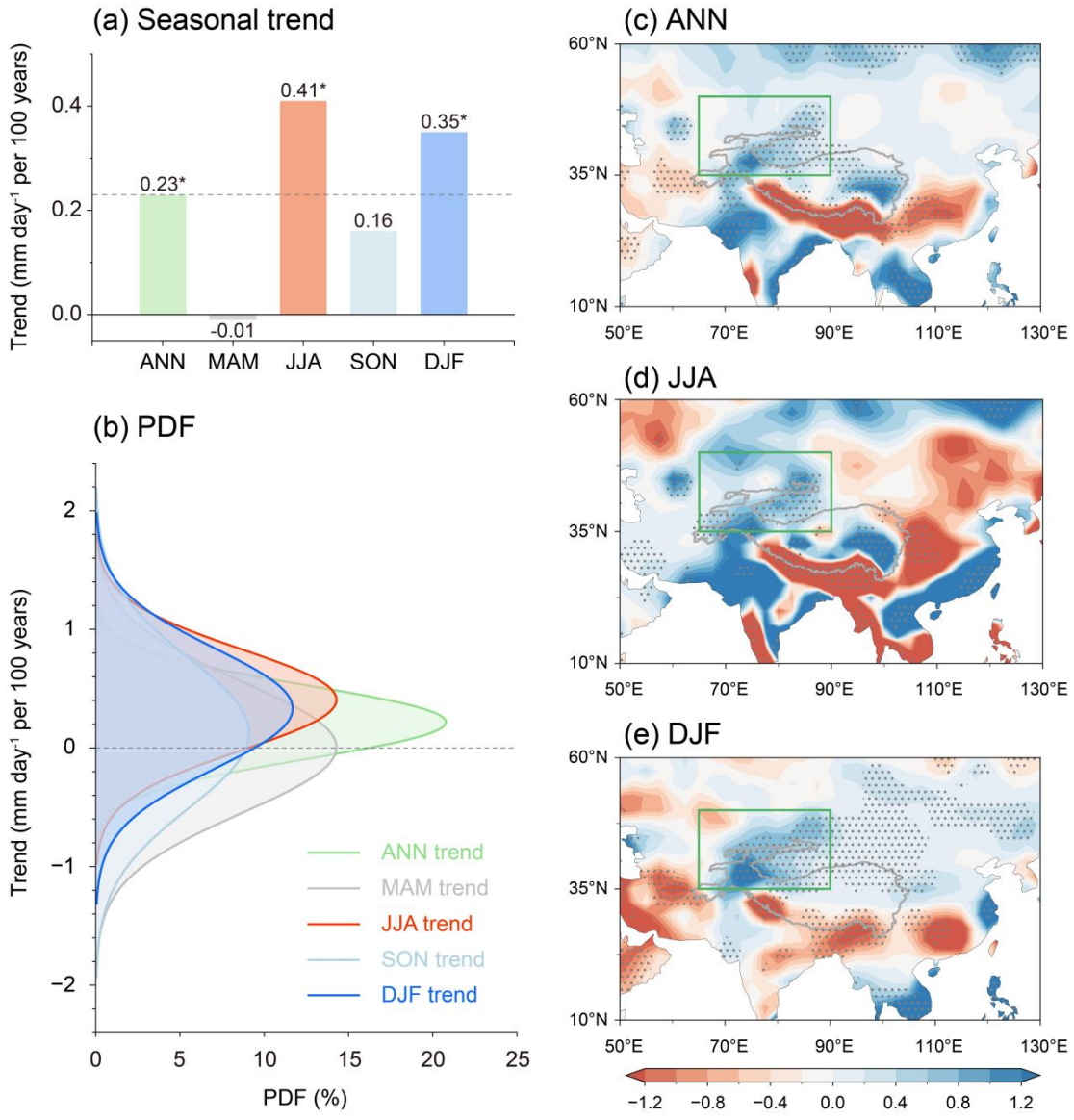

Figure 1. Seasonal precipitation trends over Central Asia derived from GPCP (1979–2014). (**a**) The trend (mm day^{-1} per 100 years) of regionally averaged precipitation for annual (January–December, ANN), spring (March–May, MAM), summer (June–August, JJA), autumn (September–November, SON), and winter (December–February, DJF). (**b**) Probability density functions (PDFs) of seasonal precipitation trends, derived from trend values at all grid points within the study area and fitted with a

normal distribution. Spatial distributions of precipitation trends for (**c**) ANN, (**d**) JJA, and (**e**) DJF. Black stars in (**a**) and gray stippling in (**c–e**) indicate trends that are statistically significant at the 90% confidence level based on a standard *t*-test. The region of Central Asia (35°N–50°N, 65°E–90°E) is delineated by thick green boxes and the thick gray curves denote Tibetan Plateau terrain height > 2500 m in (**c–e**).

3.2 Responses of seasonal precipitation to external forcings

To investigate the influence of different external forcings on seasonal precipitation, we utilize the sensitivity experiments of global-scale and regional aerosol forcings from PDRMIP. Figure 2 shows the responses of regional average precipitation to external forcings during winter and summer in Central Asia. Under global-scale forcings, winter precipitation in Central Asia is significantly increased by 24% for CO_2x2, 8% for CH_4x3, and 25% for Solar+2%, likely dependent on the magnitude of ERF induced by these three forcings. All the nine models exhibit a positive trend of winter precipitation, despite differences in precipitation magnitude. Meanwhile, the multi-model mean shows a small and insignificant decrease in summer precipitation. In contrast, summer precipitation over Central Asia exhibits a significant 15% increase induced by Sulx10Asia forcing, whereas a 13% decrease is induced by BCx10Asia forcing. The changes in aerosols lead to a negligible change in winter precipitation. We further examine the spatial distribution of seasonal precipitation changes induced by individual external forcings. As shown in Fig. 3, the CO_2x2 (Fig. 3a), CH_4x3 (Fig. 3b), and Solar+2% (Fig. 3c) forcings all yield increased winter precipitation across Central Asia. During summer, Sulx10Asia forcing increases precipitation in Central Asia (Fig. 3d), whereas BCx10Asia forcing reduces precipitation across most regions (Fig. 3e). Furthermore, we examine the influences of individual forcings on spring and autumn precipitation (Supplement Fig. S5). It shows that the global forcings increase spring precipitation in Central Asia, while BC aerosols significantly suppress spring precipitation. BC aerosols over the Tibetan Plateau increase surface temperature and enhance the plateau heat source, thereby inducing compensatory downdrafts and decreasing precipitation over arid Central Asia (Supplement Fig. S6; Qian et al., 2015; Shi et al., 2019; Xie et al., 2020a). The offsetting effects of BC aerosols may explain the spring precipitation decrease over Central Asia. The autumn precipitation response to external forcings is consistent with that in summer, indicating that sulfate aerosols increase precipitation and BC aerosols decrease precipitation. Results from the sensitivity experiments suggest pronounced seasonal differences in the drivers of precipitation change in Central Asia. The winter precipitation change is dominated by global-scale forcings whereas the summer precipitation change is primarily affected by regional aerosol forcings.

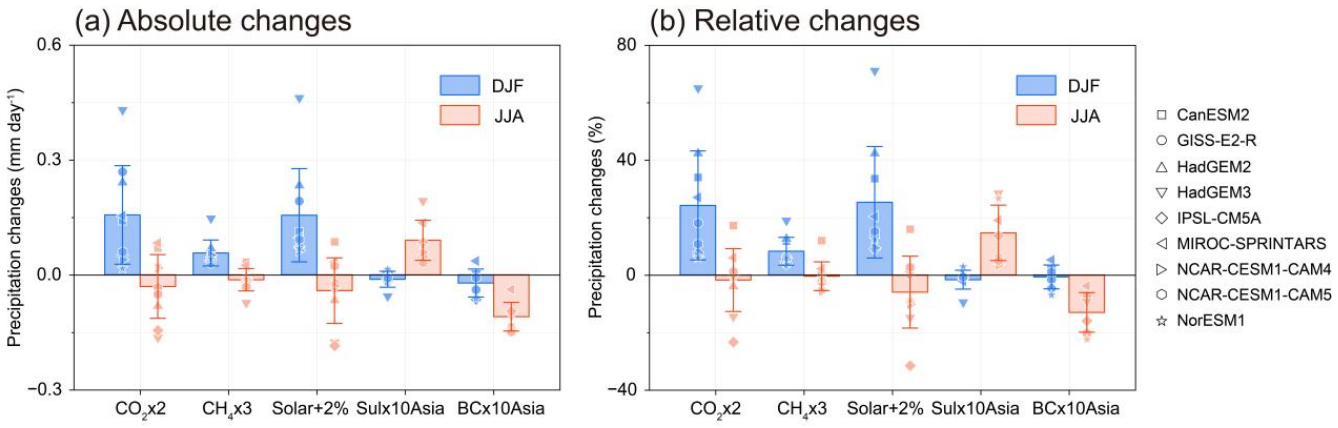

200 **Figure 2.** Seasonal precipitation responses to CO_2x2, CH_4x3, Solar+2%, Sulx10Asia, and BCx10Asia forcings during DJF and JJA over Central Asia in PDRMIP. (**a)** Absolute changes in precipitation (mm day^{-1}) over Central Asia. (**b)** Relative changes in precipitation (%) over Central Asia. Bars represent the multi-model mean across PDRMIP models, and error bars indicate ±1 inter-model standard deviation.

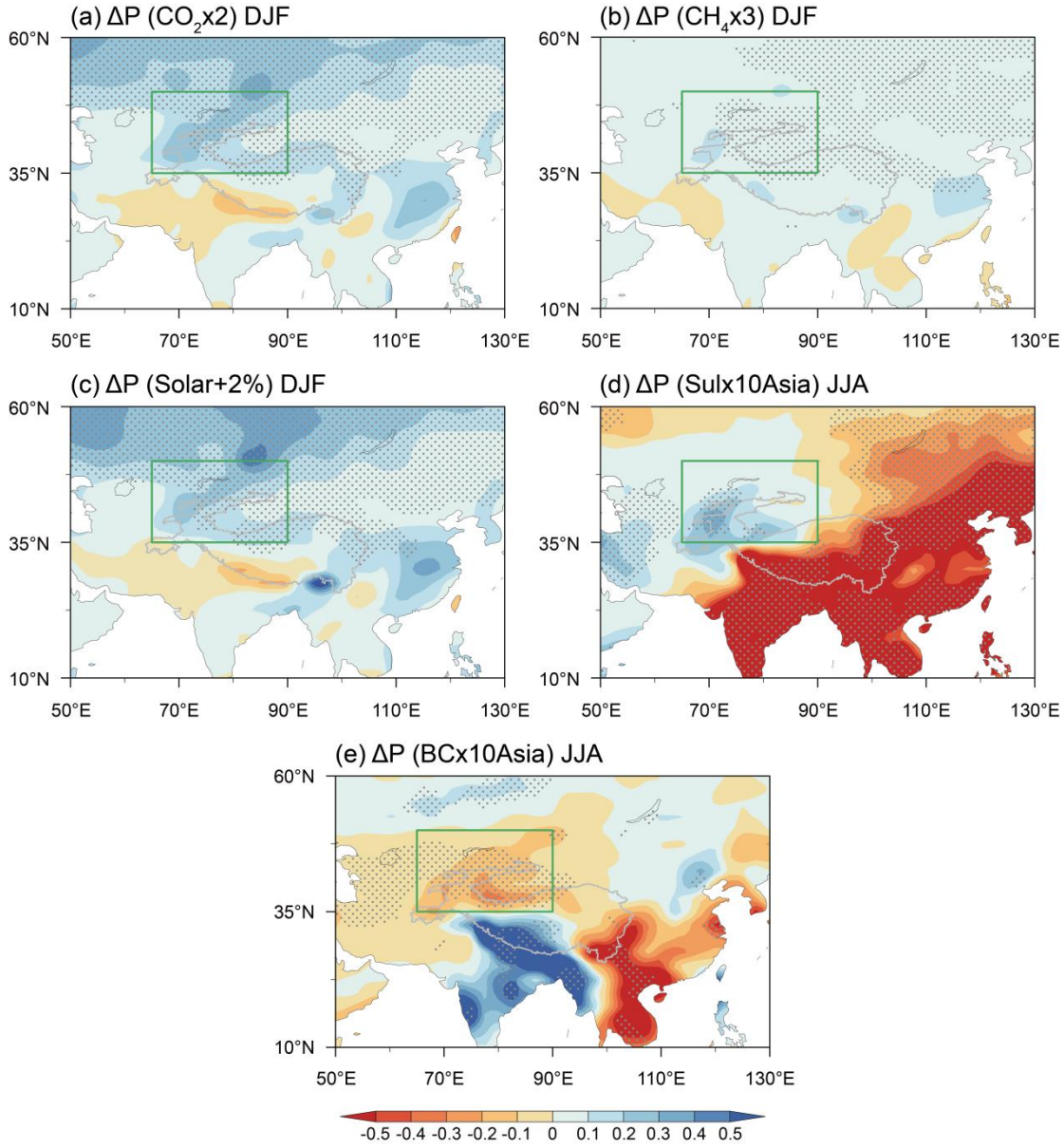

Figure 3. Spatial distributions of precipitation responses to CO_2x2, CH_4x3, Solar+2%, Sulx10Asia, and BCx10Asia forcings in PDRMIP. Multi-model mean precipitation changes (mm day^{-1}) in DJF under (**a**) CO_2x2, (**b**) CH_4x3, and (**c**) Solar+2% forcings, and in JJA under (**d**) Sulx10Asia and (**e**) BCx10Asia forcings. The region of Central Asia is delineated by thick green boxes. Thick gray curves denote Tibetan Plateau terrain height > 2500 m. The areas with gray stippling indicate regions where the PDRMIP multi-model mean changes exceed 1 standard deviation away from zero.

Next, we examine the resultant physical mechanisms of seasonal precipitation changes. In winter, CO_2x2, CH_4x3, and Solar+2% forcings induce relatively uniform ERF patterns with positive values (Supplement Figs. S7a, S7c, and S7e). The positive ERF leads to tropospheric warming (Supplement Figs. S7b, S7d, and S7f), featuring significant temperature increases in high latitudes of the Northern Hemisphere (Shindell et al., 1999; Gillett et al., 2008). Through intensifying supplies of atmospheric water vapor, the warming caused by the global-scale forcings results in statistically significant increases in vertically integrated water vapor (Figs. 4a, 4c, and 4e), enhancing winter precipitation in Central Asia (Figs. 3a–3c; Allen and Ingram, 2002; Held and Soden, 2006; Seager et al., 2010; Xue et al., 2022). The low-level tropospheric circulation responses are relatively weak, with insignificant changes of 700 hPa wind fields (Figs. 4b, 4d, and 4f). In summer, GHGs also induce a positive ERF and global warming (Supplement Fig. S8), which increases the supply of atmospheric water vapor. Note that large-scale circulations, such as the Asian summer monsoon, play a crucial role in influencing regional precipitation. Several studies suggest that large-scale circulation may weaken under global warming, which may suppress regional precipitation (Kjellsson, 2015; Xie et al., 2020b; Zhou et al., 2024). The offset between thermodynamic and dynamic effects may result in the relatively weak response in Central Asian summer precipitation under GHG forcing. Our results indicate that GHGs and solar irradiance forcings enhance winter precipitation over Central Asia primarily through thermodynamic processes under global warming.

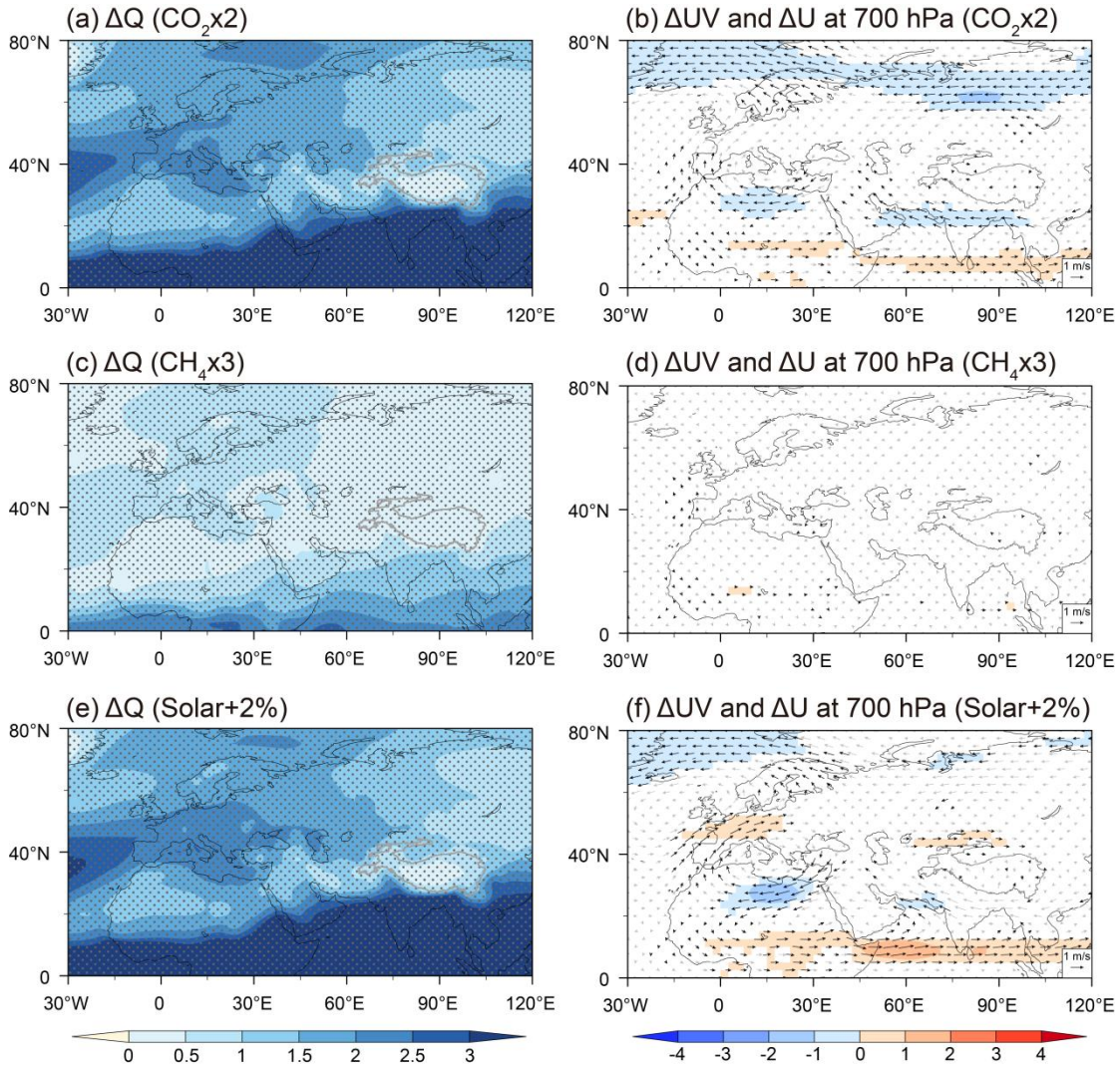

Figure 4. Multi-model mean anomalies during DJF induced by CO_2x2, CH_4x3, and Solar+2% forcings in PDRMIP. (**a**) Anomalies of vertically integrated (surface-300 hPa) water vapor (ΔQ, kg m^{-2}) and (**b**) the wind field and zonal wind at 700 hPa under CO_2x2 forcing. (**c, d**) Same as (**a, b**) but for CH_4x3 forcing. (**e, f**) Same as (**a, b**) for Solar+2% forcing. In (**a, c, e**), gray stippled regions indicate where the multi-model mean exceeds 1 standard deviation from zero. In (**b, d, f**), black arrows and colored contours denote wind field and zonal wind anomalies, respectively, where the multi-model mean exceeds 1 standard deviation away from zero. The thick gray curves denote Tibetan Plateau terrain height > 2500 m.

However, in summer, changes in Central Asian precipitation are primarily associated with the adjustment of large-scale circulation due to regional aerosol forcings. Under Sulx10Asia forcing, increased sulfate aerosols over Asia produce a regionally negative ERF and pronounced cooling across mid-latitude regions in Supplement Figs. S9a and S9b. The mid-latitude cooling alters the meridional temperature gradient, induces a southward shift of the westerly jet, and subsequently strengthens westerly winds in low-latitude regions, which influences moisture transport (Xie et al., 2022; Guo et al., 2024). As shown in the spatial distribution of vertically integrated water vapor (Fig. 5a) and moisture

flux changes (Supplement Fig. S10a), the enhanced westerlies transport more atmospheric moisture over the Atlantic Ocean to northern Africa, Central Asia, and the arid northwest of China (Figs. 5b and 5c). Atmospheric circulation changes also facilitate the transport of water vapor from the Indian Ocean into Central Asia (Zhao et al., 2014; Peng and Zhou, 2017; Wei et al., 2017; Yang et al., 2020; Xie et al., 2022). The enhanced moisture transport to Central Asia and increased moisture flux convergence over the region increases the summer precipitation (Supplement Fig. S10b and Fig. 3d), especially convective precipitation (Xie et al., 2022). Contrary to sulfate aerosol forcing, increased Asian BC aerosols absorb shortwave radiation, producing a positive ERF over Asia (Supplement Fig. S9c) and significant warming across Northern Hemisphere mid-latitudes (Supplement Fig. S9d). These changes induce a northward shift of the westerly jet and a weakening of the westerlies in the low-latitude regions (Figs. 5e and 5f), which suppress moisture transport from the Atlantic into Central Asia and reduce regional moisture flux convergence (Supplement Figs. S10c, S10d and Fig. 5d), leading to decreased summer precipitation (Fig. 3e). This suggests that Asian BC forcing might partially offset the precipitation increases caused by increased Asian sulfate aerosols. Our results suggest that the summer precipitation changes in Central Asia are mainly determined by the dynamical responses to Asian anthropogenic aerosols.

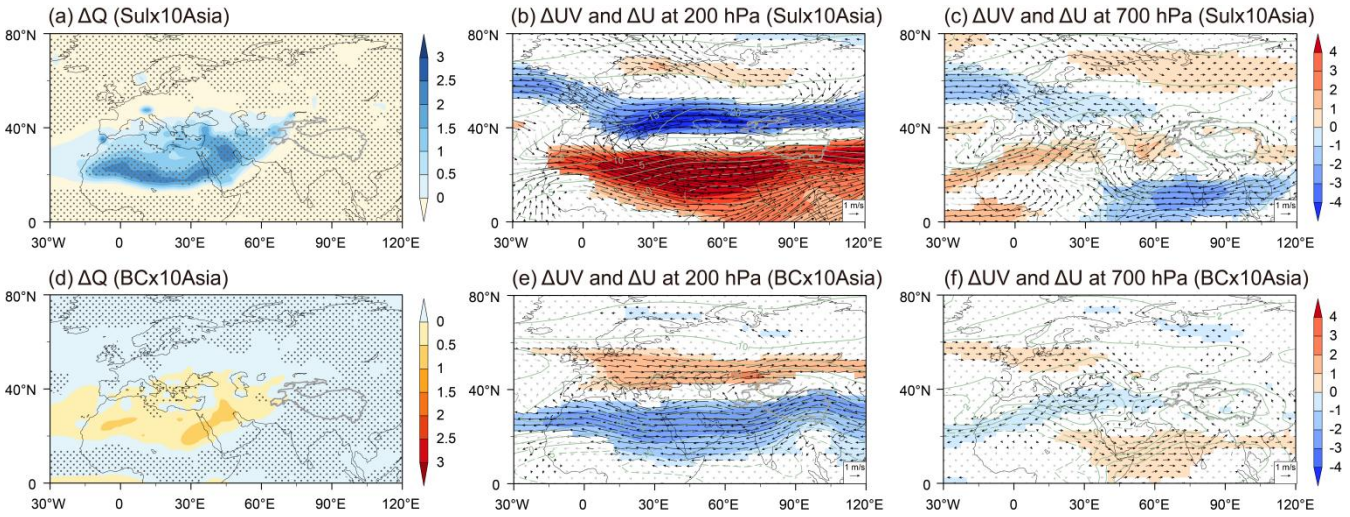

Figure 5. Multi-model mean anomalies during JJA induced by Sulx10Asia and BCx10Asia forcings in PDRMIP. (**a**) Anomalies of vertically integrated (surface–300 hPa) water vapor (ΔQ, kg m^{-2}), (**b**) wind field (ΔUV vector, m s^{-1}) and zonal wind (ΔU shading, m s^{-1}) at 200 hPa, and (**c**) wind field and zonal wind at 700 hPa under Sulx10Asia forcing. (**d**–**f**) Same as (**a**–**c**) but for BCx10Asia forcing. The gray stippled regions in (**a, d**), the black arrows in (**b, c, e, f**), and the colored contours in (**b, c, e, f**) indicate regions where the PDRMIP multi-model mean anomalies exceed 1 standard deviation away from zero. The green curves in **(b, c, e, f)** represent zonal wind climatology derived from baseline experiments in PDRMIP. The thick gray curves denote Tibetan Plateau terrain height > 2500 m.

3.3 Historical attributions and future projections of seasonal precipitation

The DAMIP simulations in CMIP6 are employed to further examine potential seasonal differences in the drivers of historical precipitation increases over Central Asia. Figure 6 shows the simulated trends in winter and summer precipitation over Central Asia (1979–2014) under individual forcings. All-forcing historical simulations exhibit an increasing winter precipitation trend of 0.28 mm day^{-1} per 100 years (Fig. 6a). This increasing trend in winter precipitation is close to the observed result (0.35 mm day^{-1} per 100 years). The individual forcing simulations indicate that GHG-induced changes dominate the increase in Central Asian winter precipitation, with 0.24 mm day^{-1} per 100 years, while anthropogenic aerosol and natural forcings induce small negative trends. The spatial distribution of precipitation trends also indicates that the GHGs mainly determine the winter precipitation increase in Supplement Figs. S11a–S11d. Figure 6b shows that all-forcing historical simulations exhibit an increasing trend of Central Asian summer precipitation with a linear trend of 0.26 mm day^{-1} per 100 years. CMIP6 multi-model ensembles underestimate summer precipitation increases by 37% relative to observations (0.41 mm day^{-1} per 100 years). Anthropogenic aerosols increase the summer precipitation the most, by 0.19 mm day^{-1} per 100 years, followed by GHGs (0.14 mm day^{-1} per 100 years) and natural forcing (0.04 mm day^{-1} per 100 years). As shown in the spatial distribution of precipitation trends (Supplement Figs. S11e–S11h), anthropogenic aerosols are the primary driver of summer precipitation increases in Central Asia. In Figure 6, dots denote the trends in regionally averaged precipitation from individual models. Results from individual models show that most models exhibit increasing precipitation trends under hist-GHG forcing in winter and under hist-aer forcing in summer. These DAMIP results indicate recent increases in winter and summer precipitation over Central Asia and significant seasonal differences in precipitation drivers, which support the results of idealized sensitivity experiments in PDRMIP.

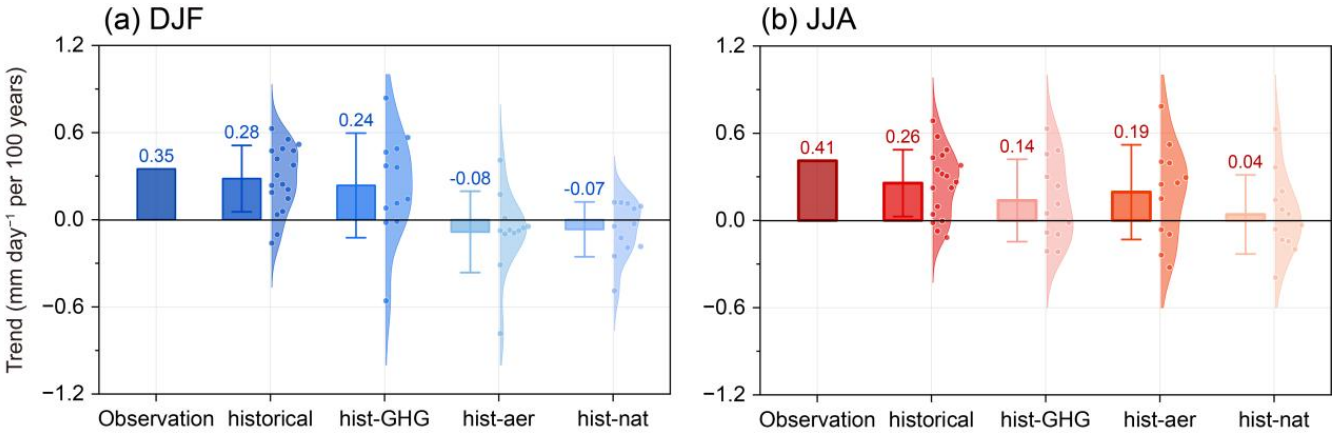

Figure 6. Central Asian seasonal precipitation trends in observations and DAMIP (1979−2014). (**a)** Central Asian DJF precipitation trend (mm day^{-1} per 100 years). (**b)** Central Asian JJA precipitation trend. Bars represent the multi-model mean precipitation trend, and error bars represent ±1 inter-model standard deviation. Dots represent the trends in regionally averaged precipitation from individual models, and curves show kernel density estimates of the trend distribution, with the bandwidth selected using Scott's rule.

To project future seasonal precipitation, we utilize the ScenarioMIP in CMIP6 to investigate the changes of precipitation in Central Asia under SSP2-45, SSP3-70, and SSP5-85 scenarios during 2015–2100. These scenarios represent different future changes in GHGs and anthropogenic aerosols (O'Neill et al., 2017; Rao et al., 2017; Samset et al., 2019; Turnock et al., 2020; Wilcox et al., 2020), with increasing GHG concentrations of different magnitudes and scenario-dependent aerosol changes. Asian aerosol decreases are more pronounced in SSP2-45 and SSP5-85, whereas SSP3-70 shows relatively weak aerosol reductions. Note that SSP3-70 is forced with nearly constant (or even increasing) aerosol forcing in some regions, such as South Africa and South America (Lund et al., 2019). Under the "middle of the road" pathway of SSP2-45, despite moderate climate mitigation measures, GHG concentrations increase continuously, inducing a significant winter precipitation increase across Central Asia (Fig. 7a). Under high GHG emission scenarios (SSP3-70 and SSP5-85), Central Asia exhibits a larger increase in winter precipitation compared to SSP2-45 (Figs. 7b and 7c). As shown in Figs. 9a–9d, the magnitude of these increasing trends is likely dependent on the GHG emission levels, with the value of 0.16 mm day^{-1} per 100 years for SSP245, 0.35 mm day^{-1} per 100 years for SSP370, and 0.44 mm day^{-1} per 100 years for SSP585 scenarios. The relative changes in winter precipitation per decade also show a wetting trend across Central Asia, with the most drastic increases found in the arid region of northwestern China (Figs. 7d–7f). Furthermore, it shows a significant reduction of summer precipitation in most regions of Central Asia under future emission scenarios (Fig. 8). The regional precipitation reduction is likely driven by the future reduction of anthropogenic aerosol emissions over Asia (mainly including East Asia and South Asia) owing to the projected implementation of Asian clean air policies (O'Neill et al., 2017; Rao et al., 2017; Wilcox et al., 2020). Regionally averaged summer precipitation over Central Asia (Figs. 9e–9h) shows smaller future changes compared to those for winter season. Our results indicate, under the SSP2-45, SSP3-70, and SSP5-85 scenarios, that Central Asian winter precipitation increases significantly in the future while summer precipitation decreases in most regions, likely due to distinct external drivers.

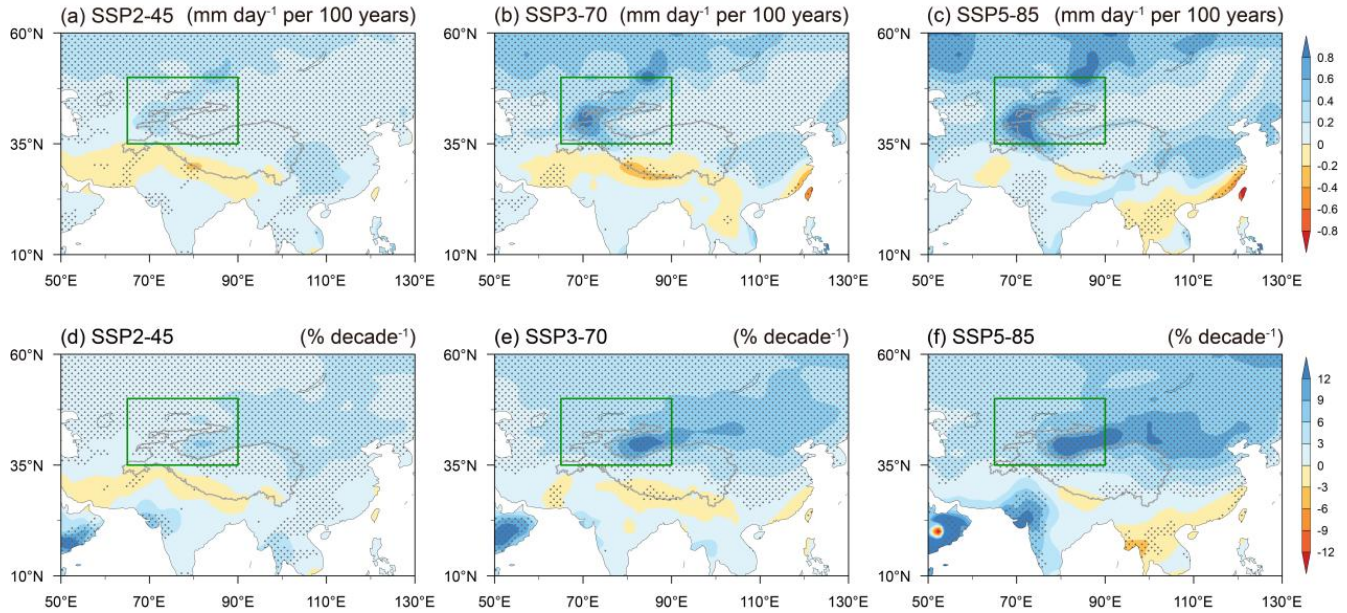

Figure 7. Spatial distribution of DJF precipitation trends over Central Asia derived from ScenarioMIP simulations. DJF precipitation trends (mm day^{-1} per 100 year) under (**a**) SSP2-45, (**b**) SSP3-70, and (**c**) SSP5-85 scenarios for 2015–2100. (**d**–**f**) Same as (**a**–**c**), but showing the trend (% decade^{-1}) as the percentage change relative to the 2015–2034 DJF climatological mean. Thick green boxes delineate the region of Central Asia. Thick gray curves denote Tibetan Plateau terrain height > 2500 m. Gray stippled regions indicate where at least 70% of models agree on the sign of the trend.

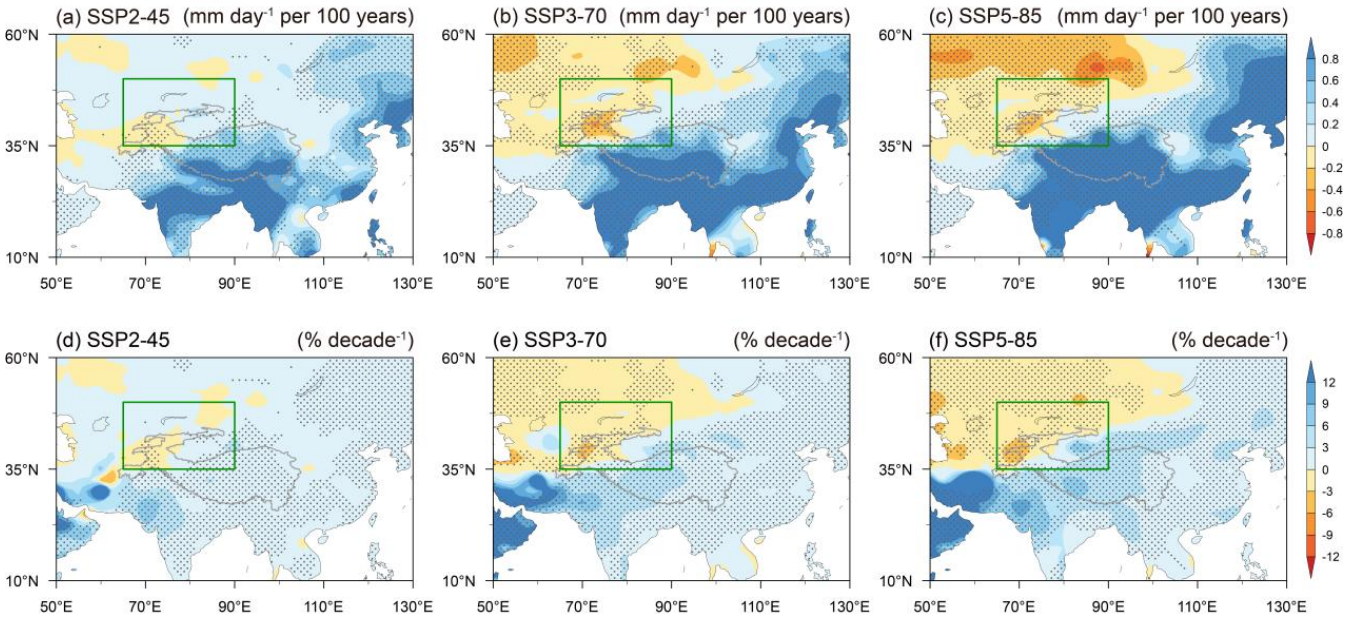

Figure 8. Spatial distribution of JJA precipitation trends over Central Asia derived from ScenarioMIP simulations. JJA precipitation trends (mm day^{-1} per 100 year) under (**a**) SSP2-45, (**b**) SSP3-70, and (**c**) SSP5-85 scenarios for 2015–2100. (**d**–**f**) Same as (**a**–**c**), but showing the trend (% decade^{-1}) as the percentage change relative to the 2015–2034 JJA climatological mean. Thick green boxes delineate the region of Central Asia. Thick gray curves denote Tibetan Plateau terrain height > 2500 m. Gray stippled regions indicate where at least 70% of models agree on the sign of the trend.

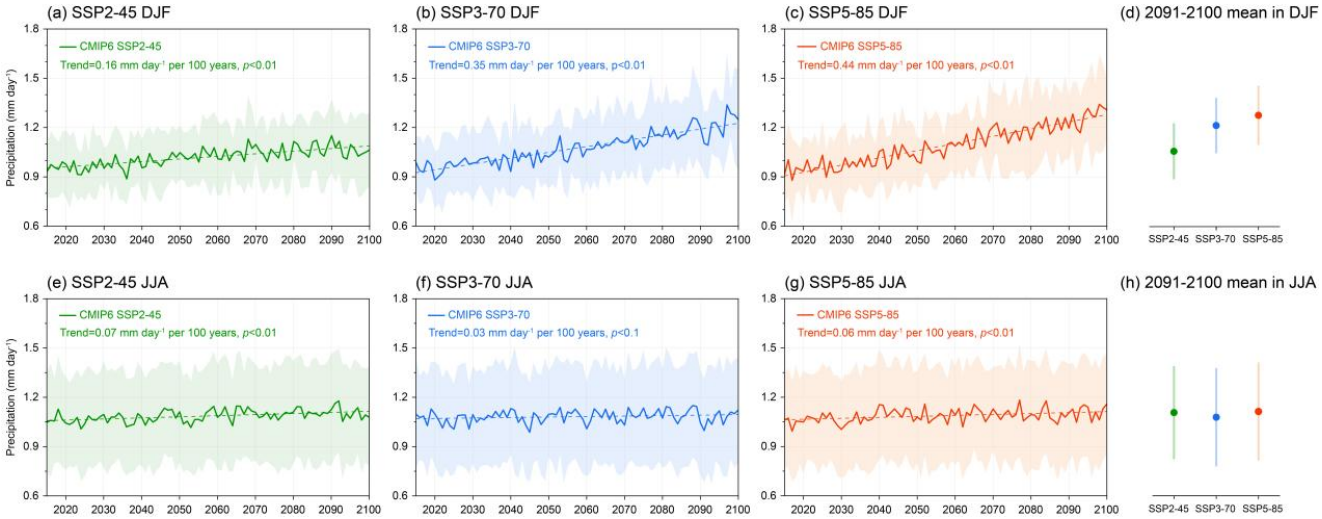

Figure 9. Seasonal precipitation over Central Asia derived from ScenarioMIP simulations. Time series of simulated Central Asian DJF precipitation (mm day^{-1}) in (**a**) SSP2-45, (**b**) SSP3-70, and (**c**) SSP5-85 (2015–2100). (**d**) Climatological mean of DJF precipitation over Central Asia for 2091–2100 under SSP2-45, SSP3-70, and SSP5-85 scenarios. (**e−h)** Same as (**a−d**) but for JJA precipitation. Solid lines in **(a−c)** and **(e−f)** represent the multi-model mean of the regional-mean precipitation over Central Asia. Dashed lines represent the linear trend (mm day^{-1} per 100 years) in precipitation and shading indicates ±1 inter-model standard deviation. Vertical lines in **(d)** and **(h)** indicate ±1 inter-model standard deviation of the 2091–2100 climatological mean precipitation over Central Asia.

4 Conclusions and discussion

Central Asia is a typical arid and semi-arid region characterized by scarce precipitation, where the regional precipitation changes profoundly impact local ecological stability, agricultural production, and socio-economic development under global climate change. Observational evidence indicates that Central Asia has experienced significant wetting in recent decades, with the most substantial increases occurring during winter and summer. In this study, we examine the impacts of external forcings on seasonal precipitation over Central Asia and the associated mechanisms using multi-model single-forcing sensitivity experiments from PDRMIP. The CO_2x2, CH_4x3, and Solar+2% forcings mainly increase winter regional precipitation through warming-induced atmospheric moisture enhancement. In summer, the Sulx10Asia forcing enhances the precipitation through shifting the westerly jet southward and intensifying westerlies at lower latitudes, which strengthens atmospheric moisture transport into the region. BCx10Asia tends to yield an opposite effect relative to Sulx10Asia, in that it partially counteracts the sulfate-induced summer precipitation increase. The CMIP6 historical attribution analysis supports the PDRMIP results, showing that GHGs primarily increase winter

precipitation and anthropogenic aerosol emissions increase summer precipitation. CMIP6 future projections further suggest that Central Asian winter precipitation is projected to continue to increase under the SSP2-45, SSP3-70, and SSP5-85 scenarios, likely associated with increasing GHG concentrations, whereas summer precipitation is projected to decrease in most regions and may be influenced by reductions in sulfate aerosol emissions under these SSP scenarios. Our results indicate that the driving factors of the observed increased precipitation in Central Asia exhibit seasonal differences, and future precipitation has divergent trends in winter and summer.

The CMIP6 historical simulations show that the models do capture positive seasonal precipitation trends over Central Asia, although these trends are underestimated (particularly for summer precipitation). The positive historical summer precipitation trend is underestimated by about 37% relative to the observations. Note that the CMIP5 models were found to severely underestimate the Asian aerosol optical depth, especially over eastern China and South Asia (Allen et al., 2013; Sanap et al., 2014; Cherian and Quaas, 2020). Despite significant improvements of CMIP6 models in simulating aerosols compared to CMIP5 (Eyring et al., 2016), the model biases of Asian aerosol persistently exist (Li et al., 2021; Fan et al., 2022; Jaisankar et al., 2024), contributing to the underestimation of the summer precipitation trend. In addition, several previous studies have shown that internal variability, such as interdecadal variations in Atlantic and Pacific sea surface temperatures, also influences precipitation trends in Central Asia (Huang et al., 2013; Gerlitz et al., 2016; Jiang et al., 2021; Yao et al., 2025). However, multi-model means are known to underestimate internal variability and its impacts on regional climate change (O'Reilly et al., 2021; Yao et al., 2024; Guinaldo et al., 2025). To further examine the influence of internal variability on precipitation trends over Central Asia, we analyze three CMIP6 large-ensemble models, including ACCESS-ESM1-5 (40 members), CanESM5 (40 members), and MIROC6 (50 members). The externally forced signal is calculated from the mean of all ensemble members, and internal variability is calculated from the deviation of each ensemble member from the ensemble mean (Wu et al., 2021). Supplement Fig. S12 shows substantial differences in precipitation trends attributable to internal variability among the three models, suggesting that internal variability has a non-negligible impact on the estimated winter and summer precipitation variations during 1979–2014. Our results suggest that, in addition to internal variability, GHGs and anthropogenic aerosols are important external forcings for the recent increase in precipitation over Central Asia.

This study is mainly based on the PDRMIP and DAMIP single-forcing sensitivity experiments to assess the historical precipitation changes in Central Asia, which makes it difficult to capture the potential impact of nonlinearity among different forcings on regional precipitation. Previous studies have shown that the nonlinear effects between CO_2 and anthropogenic aerosols can significantly influence the regional seasonal precipitation (Deng et al., 2020; Herbert et al., 2021). Further work is needed to assess how nonlinear effects impact seasonal precipitation in Central Asia.

Additionally, future seasonal precipitation changes in Central Asia are projected based on different CMIP6 emission scenarios. It is noted that the CMIP6 SSP emission scenarios underestimate the actual reduction of anthropogenic aerosols during recent decades in China (Wang et al., 2021; Ali et al., 2022), and the bias between scenario assumptions and actual reductions may hold on until mid-21st century projections (Wang et al., 2021). Since the early 2010s, anthropogenic aerosol optical depth (AOD) in East Asia has decreased markedly due to China's clean air actions and climate policies (Zheng et al., 2018; Samset et al., 2019). It shows a decreasing trend in summer precipitation over Central Asia with -0.16 mm day^{-1} per 100 years in Supplement Fig. S13, likely due to the effects induced by anthropogenic aerosol reduction. Meanwhile, the ERA5 reanalysis-based trends indicate that the Central Asian westerly jet tends to shift northward (Supplement Fig. S3). Recently, a more realistic scenario of SSP2-com from the Chinese Academy of Meteorological Sciences has been provided, derived from China's net-zero pathway (Zhong et al., 2025). We will conduct new ScenarioMIP simulations based on this scenario to improve our prediction/projection of regional climate.

Code availability

In this study, data processing was conducted using the Climate Data Operators (CDO, version 1.9.3) and the NCAR Command Language (NCL, version 6.6.2). Data visualization was performed with NCL and the open-source programming language Python (version 3.10.18). No custom code was developed. All plotting and analysis scripts are available upon request from the corresponding author.

Data availability

All data supporting the findings of this research are openly accessible. The GPCP version 2.3 monthly mean precipitation dataset is publicly available at https://psl.noaa.gov/data/gridded/data.gpcp.html. The CRU monthly land precipitation data set is available at https://crudata.uea.ac.uk/cru/data/hrg/cru_ts_4.05/cruts.2103051243.v4.05/pre/. The monthly

precipitation of the GPCC is available at https://downloads.psl.noaa.gov//Datasets/gpcc/full_v2020/precip.mon.total.0.25x0.25.v2020.nc. The ERA5 reanalysis data are available at https://cds.climate.copernicus.eu/datasets. The PDRMIP numerical simulation dataset can be accessed at https://doi.org/10.26050/WDCC/PDRMIP_2012-2021. CMIP6 simulation datasets used in this study were obtained from the Earth System Grid Federation (https://aims2.llnl.gov/search/cmip6/)

Author contributions

JNG and XNX produced the analysis of model results and wrote the original manuscript. GM, DS, AK, TI, AV, TT, KS, XZL, ZGS, YL, XDL, and HY assisted data analyses and contributed to the commenting of the results and revising of the manuscript.

Competing interests

At least one of the (co-)authors is a member of the editorial board of Atmospheric Chemistry and Physics.

Financial support

This research has been supported by the Strategic Priority Research Program of Chinese Academy of Science and the National Key R&D Program of China (2023YFF0804804). Xiaoning Xie is supported by the National Natural Science Foundation of China (42175059 and 42575054). Ke Shang is supported by the National Natural Science Foundation of China (42205037). Zhengguo Shi acknowledges the support of the Youth Innovation Promotion Association of the Chinese Academy of Sciences (Y2022101). Yangang Liu is supported by the U.S. Department of Energy's Atmospheric System Research (ASR) program.

References

Adler, R. F., Huffman, G. J., Chang, A., Ferraro, R., Xie, P. - P., Janowiak, J., Rudolf, B., Schneider, U., Curtis, S., Bolvin, D., Gruber, A., Susskind, J., Arkin, P., and Nelkin, E.: The version-2 global precipitation climatology project (GPCP) monthly precipitation analysis (1979–present), J. Hydrometeorol., 4, 1147–1167, https://doi.org/10.1175/1525-7541(2003)004<1147:TVGPCP>2.0.CO;2, 2003.

Adler, R. F., Sapiano, M. R. P., Huffman, G. J., Wang, J.-J., Gu, G., Bolvin, D., Chiu, L., Schneider, U.,

Becker, A., Nelkin, E., Xie, P., Ferraro, R., and Shin, D.-B.: The Global Precipitation Climatology Project (GPCP) monthly analysis (new version 2.3) and a review of 2017 global precipitation, Atmosphere, 9, 138, https://doi.org/10.3390/atmos9040138, 2018.

Ali, M. A., Bilal, M., Wang, Y., Qiu, Z., Nichol, J. E., de Leeuw, G., Ke, S., Mhawish, A., Almazroui, M., Mazhar, U., Habtemicheal, B. A., and Islam, M. N.: Evaluation and comparison of CMIP6 models and MERRA-2 reanalysis AOD against satellite observations from 2000 to 2014 over China, Geosci. Front., 13, 101325, https://doi.org/10.1016/j.gsf.2021.101325, 2022.

Allen, M., and Ingram, W.: Constraints on future changes in climate and the hydrologic cycle, Nature, 419, 224–232, https://doi.org/10.1038/nature01092, 2002.

Allen, R. J., Norris, J. R., and Wild, M.: Evaluation of multidecadal variability in CMIP5 surface solar radiation and inferred underestimation of aerosol direct effects over Europe, China, Japan, and India, J. Geophys. Res.-Atmos., 118, 6311–6336, https://doi.org/10.1002/jgrd.50426, 2013.

Bellouin, N., Davies, W., Shine, K. P., Quaas, J., Mülmenstädt, J., Forster, P. M., Smith, C., Lee, L., Regayre, L., Brasseur, G., Sudarchikova, N., Bouarar, I., Boucher, O., and Myhre, G.: Radiative forcing of climate change from the Copernicus reanalysis of atmospheric composition, Earth Syst. Sci. Data, 12, 1649–1677, https://doi.org/10.5194/essd-12-1649-2020, 2020.

Bond, T. C., Doherty, S. J., Fahey, D. W., Forster, P. M., Berntsen, T., DeAngelo, B. J., Flanner, M. G., Ghan, S., Kärcher, B., Koch, D., Kinne, S., Kondo, Y., Quinn, P. K., Sarofim, M. C., Schultz, M. G., Schulz, M., Venkataraman, C., Zhang, H., Zhang, S., Bellouin, N., Guttikunda, S. K., Hopke, P. K., Jacobson, M. Z., Kaiser, J. W., Klimont, Z., Lohmann, U., Schwarz, J. P., Shindell, D., Storelvmo, T., Warren, S. G., and Zender, C. S.: Bounding the role of black carbon in the climate system: A scientific assessment, J. Geophys. Res.-Atmos., 118, 5380–5552, https://doi.org/10.1002/jgrd.50171, 2013.

Booth, B. B. B., Dunstone, N. J., Halloran, P. R., Andrews, T., and Bellouin, N.: Aerosols implicated as a prime driver of twentieth-century North Atlantic climate variability, Nature, 485, 534, https://doi.org/10.1038/nature10946, 2012.

Boucher, O., Randall, D., Artaxo, P., Bretherton, C., Feingold, G., Forster, P., Kerminen, V.-M., Kondo, Y., Liao, H., Lohmann, U., Rasch, P., Satheesh, S. K., Sherwood, S., Stevens, B., and Zhang, X. Y.: Clouds and aerosols, in: Climate Change 2013: The Physical Science Basis. Contribution of Working Group I to the Fifth Assessment Report of the Intergovernmental Panel on Climate Change, edited by: Stocker, T. F., Qin, D., Plattner, G.-K., Tignor, M., Allen, S. K., Boschung, J., Nauels, A., Xia, Y., Bex, V., and Midgley, P. M., Cambridge University Press, 571–657,

https://doi.org/10.1017/CBO9781107415324.016, 2013.

Chen, F., Huang, W., Jin, L., Chen, J., and Wang, J.: Spatiotemporal precipitation variations in the arid Central Asia in the context of global warming, Sci. China Earth Sci., 54, 1812–1821, https://doi.org/10.1007/s11430-011-4333-8, 2011.

Cherian, R., and Quaas, J.: Trends in AOD, clouds, and cloud radiative effects in satellite data and CMIP5 and CMIP6 model simulations over aerosol source regions, Geophys. Res. Lett., 47, e2020GL087132, https://doi.org/10.1029/2020GL087132, 2020.

Deng, J., Dai, A., and Xu, H.: Nonlinear climate responses to increasing CO2 and anthropogenic aerosols simulated by CESM1, J. Clim., 33, 281–301, https://doi.org/10.1175/JCLI-D-19-0195.1, 2020.

Dong, B., Sutton, R. T., Shaffrey, L., and Harvey, B.: Recent decadal weakening of the summer Eurasian westerly jet attributable to anthropogenic aerosol emissions, Nat. Commun., 13, 1148, https://doi.org/10.1038/s41467-022-28816-5, 2022.

Eyring, V., Bony, S., Meehl, G. A., Senior, C. A., Stevens, B., Stouffer, R. J., and Taylor, K. E.: Overview of the coupled model intercomparison project phase 6 (CMIP6) experimental design and organization, Geosci. Model Dev., 9, 1937–1958, https://doi.org/10.5194/gmd-9-1937-2016, 2016.

Fallah, B., Russo, E., Menz, C., Hoffmann, P., Didovets, I., and Hattermann, F. F.: Anthropogenic influence on extreme temperature and precipitation in Central Asia, Sci Rep, 13, 6854, https://doi.org/10.1038/s41598-023-33921-6, 2023.

Fan, T., Liu, X., Wu, C., Zhang, Q., Zhao, C., Yang, X., and Li, Y.: Comparison of the Anthropogenic Emission Inventory for CMIP6 Models with a Country-Level Inventory over China and the Simulations of the Aerosol Properties, Adv. Atmos. Sci., 39, 80–96, https://doi.org/10.1007/s00376-021-1119-6, 2022.

Forster, P. M., Richardson, T., Maycock, A. C., Smith, C. J., Samset, B. H., Myhre, G., Andrews, T., Pincus, R., and Schulz, M.: Recommendations for diagnosing effective radiative forcing from climate models for CMIP6, J. Geophys. Res.-Atmos., 121, 12460–12475, https://doi.org/10.1002/2016JD025320, 2016.

Gerlitz, L., Vorogushyn, S., Apel, H., Gafurov, A., Unger-Shayesteh, K., and Merz, B.: A statistically based seasonal precipitation forecast model with automatic predictor selection and its application to central and south Asia, Hydrol. Earth Syst. Sci., 20, 4605–4623, https://doi.org/10.5194/hess-20-4605-2016, 2016.

Gessner, U., Naeimi, V., Klein, I., Kuenzer, C., Klein, D., and Dech, S.: The relationship between

precipitation anomalies and satellite-derived vegetation activity in Central Asia, Glob. Planet. Change, 110, 74–87, https://doi.org/10.1016/j.gloplacha.2012.09.007, 2013.

Gillett, N. P., Shiogama, H., Funke, B., Hegerl, G., Knutti, R., Matthes, K., Santer, B. D., Stone, D., and Tebaldi, C.: The detection and attribution model intercomparison project (DAMIP v1.0) contribution to CMIP6, Geosci. Model Dev., 9, 3685–3697, https://doi.org/10.5194/gmd-9-3685-2016, 2016.

Gillett, N. P., Stone, D. A., Stott, P. A., Nozawa, T., Karpechko, A. Y., Hegerl, G. C., Wehner, M. F., and Jones, P. D.: Attribution of polar warming to human influence, Nat. Geosci., 1, 750–754, https://doi.org/10.1038/ngeo338, 2008.

Guinaldo, T., Cassou, C., Sallée, J. B., and Liné, A.: Internal variability effect doped by climate change drove the 2023 marine heat extreme in the North Atlantic, Commun. Earth Environ., 6, 291, https://doi.org/10.1038/s43247-025-02197-1, 2025.

Guo, J., Xie, X., Myhre, G., Shindell, D., Kirkevåg, A., Iversen, T., Samset, B. H., Shi, Z., Li, X., Sun, H., Liu, X., and Liu, Y.: Increased Asian sulfate aerosol emissions remarkably enhance Sahel summer precipitation, Earth Future, 12, e2024EF004745, https://doi.org/10.1029/2024EF004745, 2024.

Hansen, J., Sato, M., Ruedy, R., Nazarenko, L., Lacis, A., Schmidt, G. A., Russell, G., Aleinov, I., Bauer, M., Bauer, S., Bell, N., Cairns, B., Canuto, V., Chandler, M., Cheng, Y., Del Genio, A., Faluvegi, G., Fleming, E., Friend, A., Hall, T., Jackman, C., Kelley, M., Kiang, N., Koch, D., Lean, J., Lerner, J., Lo, K., Menon, S., Miller, R., Minnis, P., Novakov, T., Oinas, V., Perlwitz, J., Perlwitz, J., Rind, D., Romanou, A., Shindell, D., Stone, P., Sun, S., Tausnev, N., Thresher, D., Wielicki, B., Wong, T., Yao, M., and Zhang, S.: Efficacy of climate forcings, J. Geophys. Res.-Atmos., 110, D18104, https://doi.org/10.1029/2005JD005776, 2005.

Harris, I., Osborn, T. J., Jones, P., and Lister, D.: Version 4 of the CRU TS monthly high-resolution gridded multivariate climate dataset, Sci. Data, 7, 109, https://doi.org/10.1038/s41597-020-0453-3, 2020.

Held, I. M., and Soden, B. J.: Robust responses of the hydrological cycle to global warming, J. Clim., 19, 5686–5699, https://doi.org/10.1175/JCLI3990.1, 2006.

Herbert, R., Wilcox, L. J., Joshi, M., Highwood, E., and Frame, D.: Nonlinear response of Asian summer monsoon precipitation to emission reductions in South and East Asia, Environ. Res. Lett., 17, 014005, https://doi.org/10.1088/1748-9326/ac3b19, 2021.

Hersbach, H., Bell, B., Berrisford, P., Hirahara, S., Horányi, A., Muñoz-Sabater, J., Nicolas, J., Peubey,

C., Radu, R., Schepers, D., Simmons, A., Soci, C., Abdalla, S., Abellan, X., Balsamo, G., Bechtold, P., Biavati, G., Bidlot, J., Bonavita, M., De Chiara, G., Dahlgren, P., Dee, D., Diamantakis, M., Dragani, R., Flemming, J., Forbes, R., Fuentes, M., Geer, A., Haimberger, L., Healy, S., Hogan, R. J., Hólm, E., Janisková, M., Keeley, S., Laloyaux, P., Lopez, P., Lupu, C., Radnoti, G., de Rosnay, P., Rozum, I., Vamborg, F., Villaume, S., and Thépaut, J.-N.: The ERA5 global reanalysis, Q. J. R. Meteorol. Soc., 146, 1999–2049, https://doi.org/10.1002/qj.3803, 2020.

Hu, Z., Zhang, C., Hu, Q., and Tian, H.: Temperature changes in Central Asia from 1979 to 2011 based on multiple datasets, J. Clim., 27, 1143–1167, https://doi.org/10.1175/JCLI-D-13-00064.1, 2014.

Hu, Z., Zhou, Q., Chen, X., Qian, C., Wang, S., and Li, J.: Variations and changes of annual precipitation in Central Asia over the last century, Int. J. Climatol., 37, 157–170, https://doi.org/10.1002/joc.4988 , 2017.

Huang, A., Zhou, Y., Zhang, Y., Huang, D., Zhao, Y., and Wu, H.: Changes of the annual precipitation over central Asia in the twenty-first century projected by multimodels of CMIP5, J. Clim., 27, 6627–6546, https://doi.org/10.1175/JCLI-D-14-00070.1, 2014.

Huang, W., Chen, F., Feng, S., Chen, J., and Zhang, X.: Interannual precipitation variations in the mid-latitude Asia and their association with large-scale atmospheric circulation, Chin. Sci. Bull., 58, 3962–3968, https://doi.org/10.1007/s11434-013-5970-4, 2013.

Jaisankar, B., Tumuluru, V. L. K., and Anandan, N. R.: Spatio-temporal correspondence of aerosol optical depth between CMIP6 simulations and MODIS retrievals over India, Environ. Sci. Pollut. Res., 31, 16899–16914, https://doi.org/10.1007/s11356-024-32314-0, 2024.

Jia, H., Ma, X., Yu, F., and Quaas, J.: Significant underestimation of radiative forcing by aerosol-cloud interactions derived from satellite-based methods, Nat. Commun., 12, 3649, https://doi.org/10.1038/s41467-021-23888-1, 2021.

Jiang, J., Zhou, T., Chen, X., and Wu, B.: Central Asian precipitation shaped by the tropical Pacific decadal variability and the Atlantic multidecadal variability, J. Clim., 34, 7541–7553, https://doi.org/10.1175/JCLI-D-20-0905.1, 2021.

Jiang, J., Zhou, T., Chen, X., and Zhang, L.: Future changes in precipitation over Central Asia based on CMIP6 projections, Environ. Res. Lett., 15, 054009, https://iopscience.iop.org/article/10.1088/1748-9326/ab7d03, 2020.

Kjellsson, J.: Weakening of the global atmospheric circulation with global warming, Clim. Dyn., 45, 975–988, https://doi.org/10.1007/s00382-014-2337-8, 2015.

Kraaijenbrink, P. D. A., Stigter, E. E., Yao, T., and Immerzeel, W. W.: Climate change decisive for

Asia's snow meltwater supply, Nat. Clim. Chang., 11, 591–597, https://doi.org/10.1038/s41558-021-01074-x, 2021.

Li, B., Chen, Y., Chen, Z., Xiong, H., and Lian, L.: Why does precipitation in northwest China show a significant increasing trend from 1960 to 2010?, Atmos. Res., 167, 275–284, https://doi.org/10.1016/j.atmosres.2015.08.017, 2016.

Li, X., Liu, Y., Wang, M., Jiang, Y., and Dong, X.: Assessment of the Coupled Model Intercomparison Project phase 6 (CMIP6) Model performance in simulating the spatial-temporal variation of aerosol optical depth over Eastern Central China, Atmos. Res., 261, 105747, https://doi.org/10.1016/j.atmosres.2021.105747, 2021.

Lioubimtseva, E., and Henebry, G. M.: Climate and environmental change in arid Central Asia: Impacts, vulnerability, and adaptations, J. Arid. Environ., 73, 963–977, https://doi.org/10.1016/j.jaridenv.2009.04.022, 2009.

Liu, L., Shawki, D., Voulgarakis, A., Kasoar, M., Samset, B. H., Myhre, G., Forster, P. M., Hodnebrog, Ø., Sillmann, J., Aalbergsjø, S. G., Boucher, O., Faluvegi, G., Iversen, T., Kirkevåg, A., Lamarque, J.-F., Olivié, D., Richardson, T., Shindell, D., and Takemura, T.: A PDRMIP multimodel study on the impacts of regional aerosol forcings on global and regional precipitation, J. Clim., 31, 4429–4447, https://doi.org/10.1175/JCLI-D-17-0439.1, 2018.

Liu, Z., Huang, J., Xiao, X., and Tong, X.: The capability of CMIP6 models on seasonal precipitation extremes over Central Asia, Atmos. Res., 278, 106364, https://doi.org/10.1016/j.atmosres.2022.106364, 2022.

Lu, Z., Zhang, Q., and Streets, D. G.: Sulfur dioxide and primary carbonaceous aerosol emissions in China and India, 1996–2010, Atmos. Chem. Phys., 11, 9839–9864, https://doi.org/10.5194/acp-11-9839-2011, 2011.

Lund, M. T., Myhre, G., and Samset, B. H.: Anthropogenic aerosol forcing under the Shared Socioeconomic Pathways, Atmos. Chem. Phys., 19, 13827–13839, https://doi.org/10.5194/acp-19-13827-2019, 2019.

Ma, Q., Zhang, J., Game, A. T., Chang, Y., and Li, S.: Spatiotemporal variability of summer precipitation and precipitation extremes and associated large-scale mechanisms in Central Asia during 1979–2018, J. Hydrol. X, 8, 100061, https://doi.org/10.1016/j.hydroa.2020.100061, 2020.

Myhre, G., Forster, P. M., Samset, B. H., Hodnebrog, Ø., Sillmann, J., Aalbergsjø, S. G., Andrews, T., Boucher, O., Faluvegi, G., Fläschner, D., Kasoar, M., Kharin, V., Kirkevåg, A., Lamarque, J.-F., Olivié, D., Richardson, T. B., Shindell, D., Shine, K. P., Stjern, C. W., Takemura, T., Voulgarakis,

A., and Zwiers, F.: PDRMIP: A precipitation driver and response model intercomparison project—Protocol and preliminary results, Bull. Am. Meteorol. Soc., 98, 1185–1198, https://doi.org/10.1175/BAMS-D-16-0019.1, 2017.

Myhre, G., Samset, B., Forster, P. M., Hodnebrog, Ø., Sandstad, M., Mohr, C. W., Sillmann, J., Stjern, C. W., Andrews, T., Boucher, O., Faluvegi, G., Iversen, T., Lamarque, J.-F., Kasoar, M., Kirkevåg, A., Kramer, R., Liu, L., Mülmenstädt, J., Olivié, D.,a Quas, J., Richardson, T. B., Shawki, D., Shindell, D., Smith, C., Stier, P., Tang, T., Takemura, T., Voulgarakis, A., and Watson-Parris, D.: Scientific data from precipitation driver response model intercomparison project, Sci. Data, 9, 123, https://doi.org/10.1038/s41597-022-01194-9, 2022.

Myhre, G., Shindell, D., Bréon, F.-M., Collins, W., Fuglestvedt, J., Huang, J., Koch, D., Lamarque, J.-F., Lee, D., Mendoza, B., Nakajima, T., Robock, A., Stephens, G., Takemura, T., and Zhang, H.: Anthropogenic and Natural Radiative Forcing, in: Climate Change 2013: The Physical Science Basis. Contribution of Working Group I to the Fifth Assessment Report of the Intergovernmental Panel on Climate Change, edited by: Stocker, T. F., Qin, D., Plattner, G.-K., Tignor, M., Allen, S. K., Boschung, J., Nauels, A., Xia, Y., Bex, V., and Midgley, P. M., Cambridge University Press, 659–740, https://doi.org/10.1017/CBO9781107415324.018, 2013.

O'Neill, B. C., Kriegler, E., Ebi, K. L., Kemp-Benedict, E., Riahi, K., Rothman, D. S., van Ruijven, B. J., van Vuuren, D. P., Birkmann, J., Kok, K., Levy, M., and Solecki, W.: The roads ahead: Narratives for shared socioeconomic pathways describing world futures in the 21st century, Glob. Environ. Change, 42, 169–180, https://doi.org/10.1016/j.gloenvcha.2015.01.004, 2017.

O'Neill, B. C., Tebaldi, C., van Vuuren, D. P., Eyring, V., Friedlingstein, P., Hurtt, G., Knutti, R., Kriegler, E., Lamarque, J.-F., Lowe, J., Meehl, G. A., Moss, R., Riahi, K., and Sanderson, B. M.: The scenario model intercomparison project (ScenarioMIP) for CMIP6, Geosci. Model Dev., 9, 3461–3482, https://doi.org/10.5194/gmd-9-3461-2016, 2016.

O'Reilly, C. H., Woollings, T., Zanna, L., and Weisheimer, A.: Projections of northern hemisphere extratropical climate underestimate internal variability and associated uncertainty, Commun. Earth Environ., 2, 194, https://doi.org/10.1038/s43247-021-00268-7, 2021.

Ohara, T., Akimoto, H., Kurokawa, J., Horii, N., Yamaji, K., Yan, X., and Hayasaka, T.: An Asian emission inventory of anthropogenic emission sources for the period 1980–2020, Atmos. Chem. Phys., 7, 4419–4444, https://doi.org/10.5194/acp-7-4419-2007, 2007.

Oki, T., and Kanae, S.: Global hydrological cycles and world water resources, Science, 313, 1068–1072, https://doi.org/10.1126/science.1128845, 2006.

Peng, D., and Zhou, T.: Why was the arid and semiarid northwest China getting wetter in the recent decades?, Geophys. Res.-Atmos., 122, 9060–9075, https://doi.org/10.1002/2016JD026424, 2017.

Peng, D., Zhou, T., Zhang, L., and Wu, B.: Human contribution to the increasing summer precipitation in Central Asia from 1961 to 2013, J. Clim., 31, 8005–8021, https://doi.org/10.1175/JCLI-D-17-0843.1, 2018.

Qian, Y., Yasunari, T. J., Doherty, S. J., Flanner, M. G., Lau, W. K. M., Ming, J., Wang, H., Wang, M., Warren, S. G., and Zhang, R.: Light-absorbing Particles in Snow and Ice: Measurement and Modeling of Climatic and Hydrological Impact, Adv. Atmos. Sci., 32, 64–91, https://doi.org/10.1007/s00376-014-0010-0, 2015.

Ramanathan, V., and Carmichael, G.: Global and regional climate changes due to black carbon, Nat. Geosci., 1, 221–227, https://doi.org/10.1038/ngeo156, 2008.

Rao, S., Klimont, Z., Smith, S. J., Van Dingenen, R., Dentener, F., Bouwman, L., Riahi, K., Amann, M., Bodirsky, B. L., van Vuuren, D. P., Aleluia Reis, L., Calvin, K., Drouet, L., Fricko, O., Fujimori, S., Gernaat, D., Havlik, P., Harmsen, M., Hasegawa, T., Heyes, C., Hilaire, J., Luderer, G., Masui, T., Stehfest, E., Strefler, J., van der Sluis, S., and Tavoni, M.: Future air pollution in the Shared Socio-economic Pathways, Glob. Environ. Change, 42, 346–358, https://doi.org/10.1016/j.gloenvcha.2016.05.012, 2017.

Reyer, C. P. O., Otto, I. M., Adams, S., Albrecht, T., Baarsch, F., Cartsburg, M., Coumou, D., Eden, A., Ludi, E., Marcus, R., Mengel, M., Mosello, B., Robinson, A., Schleussner, C.-F., Serdeczny, O., and Stagl, J.: Climate change impacts in Central Asia and their implications for development, Reg. Environ. Change, 17, 1639–1650, https://doi.org/10.1007/s10113-015-0893-z, 2017.

Rotstayn, L. D., and Lohmann, U.: Tropical rainfall trends and the indirect aerosol effect, J. Clim., 15, 2103–2116, https://doi.org/10.1175/1520-0442(2002)015<2103:TRTATI>2.0.CO;2, 2002.

Samset, B. H., Lund, M. T., Bollasina, M., Myhre, G., and Wilcox, L.: Emerging Asian aerosol patterns, Nat. Geosci., 12, 582–584, https://doi.org/10.1038/s41561-019-0424-5, 2019.

Sanap, S. D., Ayantika, D. C., Pandithurai, G., and Niranjan, K.: Assessment of the aerosol distribution over Indian subcontinent in CMIP5 models, Atmos. Environ., 87, 123-137, https://doi.org/10.1016/j.atmosenv.2014.01.017, 2014.

Schneider, U., Becker, A., Finger, P., Rustemeier, E., and Ziese, M.: GPCC full data monthly product version 2020 at 0.25°: Monthly land-surface precipitation from rain-gauges built on GTS-based and historical data, GPCC, https://doi.org/10.5676/DWD_GPCC/FD_M_V2020_025, 2020.

Seager, R., Naik, N., and Vecchi, G. A.: Thermodynamic and dynamic mechanisms for large-scale

changes in the hydrological cycle in response to global warming, J. Clim., 23, 4651–4668, https://doi.org/10.1175/2010JCLI3655.1, 2010.

Shawki, D., Voulgarakis, A., Chakraborty, A., Kasoar, M., and Srinivasan, J.: The South Asian monsoon response to remote aerosols: Global and regional mechanisms, J. Geophys. Res. Atmos., 123, 11585–11602, https://doi.org/10.1029/2018JD028623, 2018.

Shi, Z., Xie, X., Li, X., Yang, L., Xie, X., Lei, J., Sha, Y., and Liu, X.: Snow-darkening versus direct radiative effects of mineral dust aerosol on the Indian summer monsoon onset: role of temperature change over dust sources, Atmos. Chem. Phys., 19, 1605–1622, https://doi.org/10.5194/acp-19-1605-2019, 2019.

Shindell, D. T., Miller, R. L., Schmidt, G. A., and Pandolfo, L.: Simulation of recent northern winter climate trends by greenhouse-gas forcing, Nature, 399, 452–455, https://doi.org/10.1038/20905, 1999.

Shindell, D. T., Voulgarakis, A., Faluvegi, G., and Milly, G.: Precipitation response to regional radiative forcing, Atmos. Chem. Phys., 12, 6969–6982, https://doi.org/10.5194/acp-12-6969-2012, 2012.

Shindell, D., and Faluvegi, G.: Climate response to regional radiative forcing during the twentieth century, Nat. Geosci., 2, 294–300, https://doi.org/10.1038/ngeo473 , 2009.

Smith, C. J., Kramer, R. J., Myhre, G., Alterskjær, K., Collins, W., Sima, A., Boucher, O., Dufresne, J.-L., Nabat, P., Michou, M., Yukimoto, S., Cole, J., Paynter, D., Shiogama, H., O'Connor, F. M., Robertson, E., Wiltshire, A., Andrews, T., Hannay, C., Miller, R., Nazarenko, L., Kirkevåg, A., Olivié, D., Fiedler, S., Lewinschal, A., Mackallah, C., Dix, M., Pincus, R., and Forster, P. M.: Effective radiative forcing and adjustments in CMIP6 models, Atmos. Chem. Phys., 20, 9591–9618, https://doi.org/10.5194/acp-20-9591-2020, 2020.

Stjern, C. W., Samset, B. H., Myhre, G., Forster, P. M., Hodnebrog, Ø., Andrews, T., Boucher, O., Faluvegi, G., Iversen, T., Kasoar, M., Kharin, V., Kirkevåg, A., Lamarque, J.-F., Olivié, D., Richardson, T., Shawki, D., Shindell, D., Smith, C. J., Takemura, T., and Voulgarakis, A.: Rapid adjustments cause weak surface temperature response to increased black carbon concentrations, Geophys. Res.-Atmos., 122, 11462–11481, https://doi.org/10.1002/2017JD027326, 2017.

Turnock, S. T., Allen, R. J., Andrews, M., Bauer, S. E., Deushi, M., Emmons, L., Good, P., Horowitz, L., John, J. G., Michou, M., Nabat, P., Naik, V., Neubauer, D., O'Connor, F. M., Olivié, D., Oshima, N., Schulz, M., Sellar, A., Shim, S., Takemura, T., Tilmes, S., Tsigaridis, K., Wu, T., and

Zhang, J.: Historical and future changes in air pollutants from CMIP6 models, Atmos. Chem. Phys., 20, 14547–14579, https://doi.org/10.5194/acp-20-14547-2020, 2020.

Undorf, S., Polson, D., Bollasina, M. A., Ming, Y., Schurer, A., and Hegerl, G. C.: Detectable impact of local and remote anthropogenic aerosols on the 20th century changes of West African and South Asian monsoon precipitation, J. Geophys. Res.-Atmos., 123, 4871–4889, https://doi.org/10.1029/2017JD027711, 2018.

Vose, R. S., Arndt, D., Banzon, V. F., Easterling, D. R., Gleason, B., Huang, B., Kearns, E., Lawrimore, J. H., Menne, M. J., Peterson, T. C., Reynolds, R. W., Smith, T. M., Williams, C. N., Jr., and Wuertz, D. B.: NOAA's Merged Land-Ocean Surface Temperature Analysis, Bull. Am. Meteorol. Soc., 93, 1677–1685, https://doi.org/10.1175/BAMS-D-11-00241.1, 2012.

Wang, Y., Zhou, B., Qin, D., Wu, J., Gao, R., and Song, L.: Changes in mean and extreme temperature and precipitation over the arid region of northwestern China: observation and projection, Adv. Atmos. Sci., 34, 289–305, https://doi.org/10.1007/s00376-016-6160-5, 2017.

Wang, Z., Lin, L., Xu, Y., Che, H., Zhang, X., Zhang, H., Dong, W., Wang, C., Gui, K., and Xie, B.: Incorrect Asian aerosols affecting the attribution and projection of regional climate change in CMIP6 models, npj Clim. Atmos. Sci., 4, 2, https://doi.org/10.1038/s41612-020-00159-2, 2021.

Wei, W., Zhang, R., Wen, M., and Yang, S.: Relationship between the Asian westerly jet stream and summer rainfall over central Asia and North China: Roles of the Indian monsoon and the South Asian high, J. Clim., 30, 537–552, https://doi.org/10.1175/JCLI-D-15-0814.1, 2017.

Westervelt, D. M., Conley, A. J., Fiore, A. M., Lamarque, J.-F., Shindell, D. T., Previdi, M., Mascioli, N. R., Faluvegi, G., Correa, G., and Horowitz, L. W.: Connecting regional aerosol emissions reductions to local and remote precipitation responses, Atmos. Chem. Phys., 18, 12461–12475, https://doi.org/10.5194/acp-18-12461-2018, 2018.

Wilcox, L. J., Liu, Z., Samset, B. H., Hawkins, E., Lund, M. T., Nordling, K., Undorf, S., Bollasina, M., Ekman, A. M. L., Krishnan, S., Merikanto, J., and Turner, A. G.: Accelerated increases in global and Asian summer monsoon precipitation from future aerosol reductions, Atmos. Chem. Phys., 20, 11955–11977, https://doi.org/10.5194/acp-20-11955-2020, 2020.

Wu, M., Zhou, T., Li, C., Li, H., Chen, X., Wu, B., Zhang, W., and Zhang, L.: A very likely weakening of Pacific Walker Circulation in constrained near-future projections, Nat. Commun., 12, 6502, https://doi.org/10.1038/s41467-021-26693-y, 2021.

Xie, X., Duan, A., Shi, Z., Li, X., Sun, H., Liu, X., Cheng, X., Zhao, T., Che, H., and Liu, Y.: Modulation of springtime surface sensible heating over the Tibetan Plateau on the interannual

variability of East Asian dust cycle, Atmos. Chem. Phys., 20, 11143–11159, https://doi.org/10.5194/acp-20-11143-2020, 2020a.

Xie, X., Myhre, G., Liu, X., Li, X., Shi, Z., Wang, H., Kirkevåg, A., Lamarque, J.-F., Shindell, D., Takemura, T., and Liu, Y.: Distinct responses of Asian summer monsoon to black carbon aerosols and greenhouse gases, Atmos. Chem. Phys., 20, 11823–11839, https://doi.org/10.5194/acp-20-11823-2020, 2020b.

Xie, X., Myhre, G., Shindell, D., Faluvegi, G., Takemura, T., Voulgarakis, A., Shi, Z., Li, X., Xie, X., Liu, H., Liu, X., and Liu, Y.: Anthropogenic sulfate aerosol pollution in South and East Asia induces increased summer precipitation over arid Central Asia, Commun. Earth Environ., 3, 328, https://doi.org/10.1038/s43247-022-00660-x, 2022.

Xue, J., Xie, X., and Liu, X.: Differing responses of precipitation in Northern Hemisphere mid-latitudes to increased black carbon aerosols and carbon dioxide, Environ. Res., 210, 112938, https://doi.org/10.1016/j.envres.2022.112938, 2022.

Yang, H., Xu, G., Mao, H., and Wang, Y.: Spatiotemporal variation in precipitation and water vapor transport over Central Asia in winter and summer under global warming, Front. Earth Sci., 8, 297, https://doi.org/10.3389/feart.2020.00297, 2020.

Yao, M., Tang, H., and Huang, G.: Inter-model uncertainty in projecting precipitation changes over central Asia under global warming, Geophys. Res. Lett., 51, e2024GL111989, https://doi.org/10.1029/2024GL111989, 2024.

Yao, M., Tang, H., and Huang, G.: Roles of external forcing and internal variability in winter precipitation changes over Central Asia, Earth Future, 13, e2025EF006064, https://doi.org/10.1029/2025EF006064, 2025.

Yu, X., Zhao, Y., Ma, X., Yao, J., and Li, H.: Projected changes in the annual cycle of precipitation over central Asia by CMIP5 models, Int. J. Climatol., 38, 5589–5604, https://doi.org/10.1002/joc.5765, 2018.

Zhang, J., Wang, S., He, Y., Ren, Y., and Huang, J.: Contribution of the precipitation-recycling process to the wetting trend in Xinjiang, China, J. Geophys. Res.-Atmos., 127, e2021JD036407, https://doi.org/10.1029/2021JD036407, 2022.

Zhao, Y., Wang, M., Huang, A., Li, H., Huo, W., and Yang, Q.: Relationships between the West Asian subtropical westerly jet and summer precipitation in northern Xinjiang, Theor. Appl. Climatol., 116, 403–411, https://doi.org/10.1007/s00704-013-0948-3, 2014.

Zheng, B., Tong, D., Li, M., Liu, F., Hong, C., Geng, G., Li, H., Li, X., Peng, L., Qi, J., Yan, L., Zhang,

Y., Zhao, H., Zheng, Y., He, K., and Zhang, Q.: Trends in China's anthropogenic emissions since 2010 as the consequence of clean air actions, Atmos. Chem. Phys., 18, 14095–14111, https://doi.org/10.5194/acp-18-14095-2018, 2018.

Zhong, J., Zhang, X., Zhang, D., Wang, D., Guo, L., Peng, H., Huang, X., Wang, Z., Lei, Y., Lu, Y., Qu, C., Zhang, X., and Miao, C.: Plausible global emissions scenario for 2 °C aligned with China's net-zero pathway, Nat. Commun., 16, 8102, https://doi.org/10.1038/s41467-025-62983-5, 2025.

Zhou, S., Huang, P., Wang, L., Hu, K., Huang, G., and Hu, P.: Robust changes in global subtropical circulation under greenhouse warming, Nat. Commun., 15, 96, https://doi.org/10.1038/s41467-023-44244-5, 2024.